ELECTROCHEMICAL IMPEDANCE ANALYSIS OF LITHIUM COBALT OXIDE BATTERIES

By

SALIM EROL

A THESIS PRESENTED TO THE GRADUATE SCHOOL
OF THE UNIVERSITY OF FLORIDA IN PARTIAL FULFILLMENT
OF THE REQUIREMENTS FOR THE DEGREE OF
MASTER OF SCIENCE

UNIVERSITY OF FLORIDA

2011

To my parents and friends

ACKNOWLEDGMENTS

First of all, I would like to thank Dr. Mark Orazem for guiding me in my thesis with his large knowledge and experiences in electrochemical engineering field. He always has been positive and patient with me. Second, I thank to my research group members, who helped and supported me whenever I need. Last but not least, I want to thank Turkish Educational Ministry for the financial support throughout my master's program.

TABLE OF CONTENTS

page

LIST OF FIGURES

Figure page

Abstract of Thesis Presented to the Graduate School
of the University of Florida in Partial Fulfillment of the
Requirements for the Degree of Master of Science

ELECTROCHEMICAL IMPEDANCE ANALYSIS OF LITHIUM COBALT OXIDE BATTERIES

By

Salim Erol

August 2011

Chair: Mark E. Orazem
Major: Chemical Engineering

Impedance measurements on commercial $LiCoO_2$ secondary 2032 button cells are shown to be extremely sensitive to state-of-charge, overcharge, overdischarge, and elapsed time. The $LiCoO_2$ cells were initially charged under galvanostatic control to 3.80 V. Each cell was potentiostatically held at constant cell potential. After the constant-potential rest period, the impedance was measured using a 10 mV perturbation and 100 kHz – 0.02 Hz frequency range. Lissajous plots were used to ensure linearity during the impedance measurement. Following each impedance measurement, the cell potential was potentiostatically modified for the charge and discharge profiles in 0.20 V steps. In the same manner, the discharge profile analysis was executed immediately following the charge schedule. To study the influence of overcharge, the cell was initially charged under constant current to 4.20 V. Impedance measurements were performed at each 80 mV step up to and including 5.00 V. A similar protocol was followed for the overdischarge. Impedance measurements were performed at each 80 mV step down to and including 2.20 V.

After overcharging to a potential of 5 V, the battery was allowed to relax for four days at the open-circuit condition. When held at open-circuit, the overcharged battery

rapidly reached a cell potential within the nominal operating range. After overdischarging to a potential of 2.20 V, the battery was allowed to relax for four days at the open-circuit condition. When held at open-circuit, the overdischarged battery also reached a cell potential within the nominal operating range, but this process was slower. The impedance response showed a persistent change to the electrochemical characteristics of a coin cell subjected to overcharge and returned to normal cell potentials; whereas, the electrochemical characteristics returned quickly to normal for a coin cell subject to overdischarge and returned to normal cell potentials. Measurement model analysis was used to show that the change in the impedance response with elapsed time was due to a change in the Ohmic resistance.

CHAPTER 1
INTRODUCTION

Lithium-ion (Li-ion) batteries are rechargeable batteries that are used in a broad range of electronic devices. They have a higher power density as compared to other batteries such as nickel-cadmium and lead-acid.[1] When they are charged Li^+ ions leave cathode and move to anode, when they are discharged vice versa. The most common lithium-ion batteries use a $LiCoO_2$ cathode, a graphite anode, and a $LiPF_6$ electrolyte. The structure of a $LiCoO_2$ battery and movements of Li^+ ions are presented in Figure1-1.

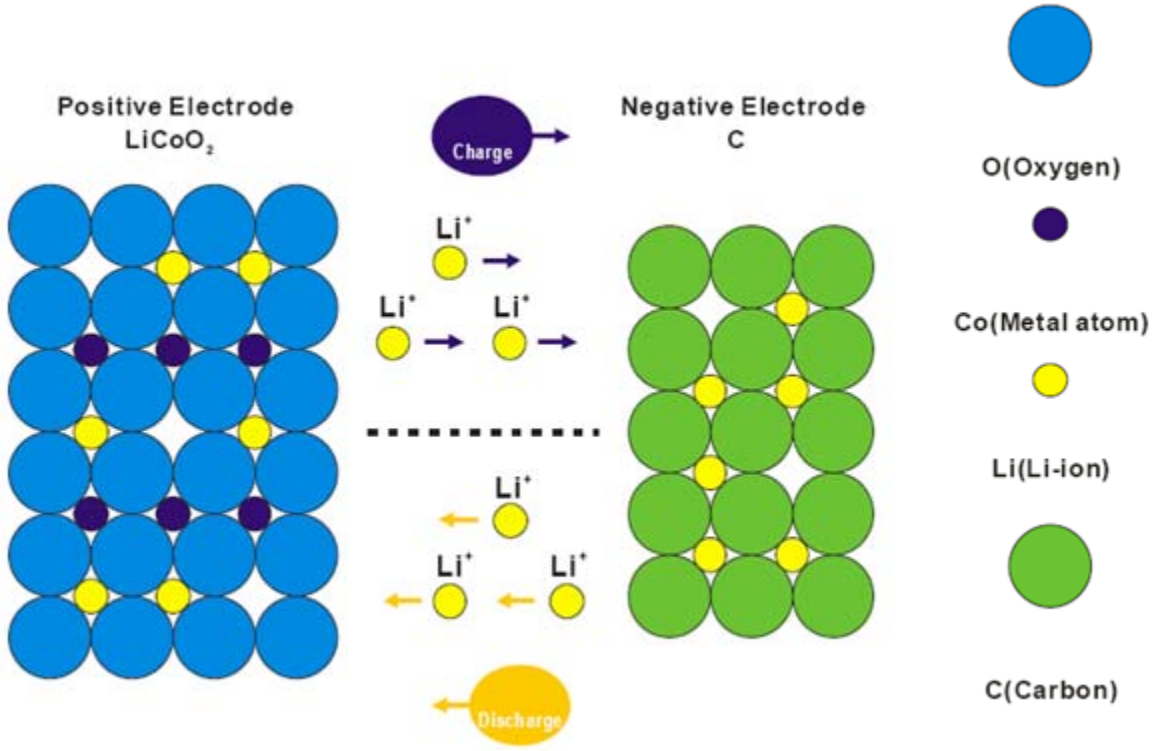

Figure 1-1. The indication of movements of Li^+ ions when a $LiCoO_2$ battery is charged and discharged

It is recognized that the cycle life of a Li-ion battery is reduced if it is overcharged or overdischarged. Urquidi-Macdonald and Bomberger[2] discussed use of artificial neural networks to predict the cycle life of Li-ion batteries. Peterson et al.[3] studied the effects of combined driving and vehicle-to-grid (V2G) usage on the lifetime performance of

relevant commercial Li-ion cells. Maleki and Howard[4] reported that overdischarging of Li-ion cells below 1.5 V may cause capacity losses and/or thermal stability changes which could impact tolerance to abuse conditions. They reported impedance diagrams which showed increased in high and low frequency asymptotes with cycle life. Belov and Yang[5] used electrical impedance spectroscopy and scanning electron microscopy to characterize electrode materials at different state-of-overcharge and overcharge conditions. A dramatic increase in resistance for the 4.6 and 5.0 V test was reported, but the interpretation was only qualitative.

CHAPTER 2
ELECROCHEMICAL IMPEDANCE SPECTROSCOPY

Impedance spectroscopy is an experimental method for analyzing and characterizing electrochemical systems. An electrochemical system, as shown in Figure 2-1, can be represented by an equivalent circuit which consists of resistances and capacitances. Here C is capacitance, R_e is ohmic resistance, and R_t is charge transfer resistance.

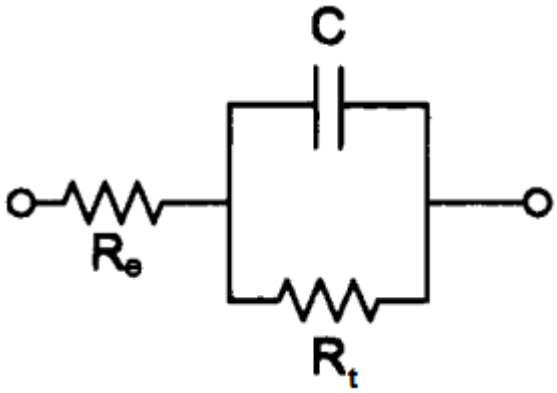

Figure 2-1. A simple electrochemical circuit representation

The impedance can basically be described as the complex ratio of oscillating potential, and current. [6]

$$Z = \frac{\tilde{V}}{\tilde{I}} = \frac{\Delta V}{\Delta I} e^{j\phi} = Z_r + jZ_j \qquad (2-1)$$

Here Z is impedance, j is a complex number equal to $\sqrt{-1}$, ϕ is the phase difference between the potential and current, and Z_r and Z_j are the real and imaginary components of the impedance, respectively. Based on the equation $(2-1)$, the electrochemical system should be perturbed by oscillating potential or current with a significantly small values which is indicated in Figure 2-2. [7]

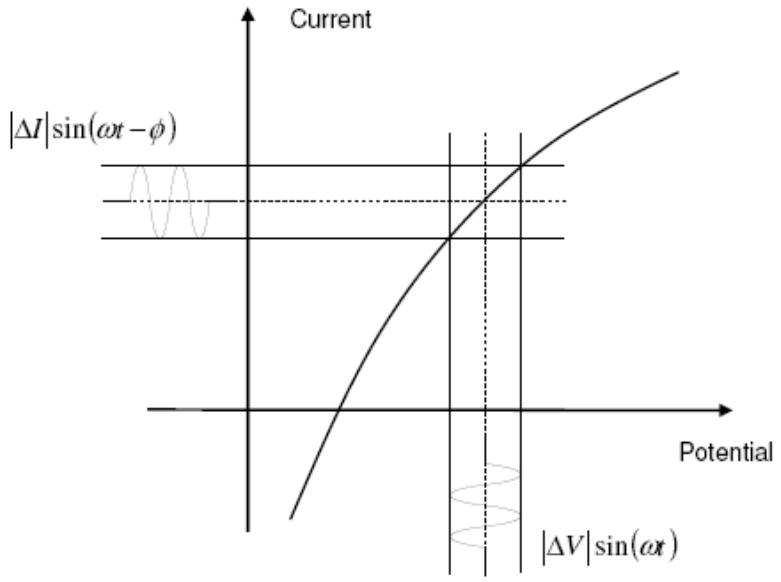

Figure 2-2. Perturbation of an electrochemical system with a small sinusoidal signal at steady state, where ΔV and ΔI represent the potential and current oscillating at the same frequency ω, and the phase difference between potential and current is ϕ

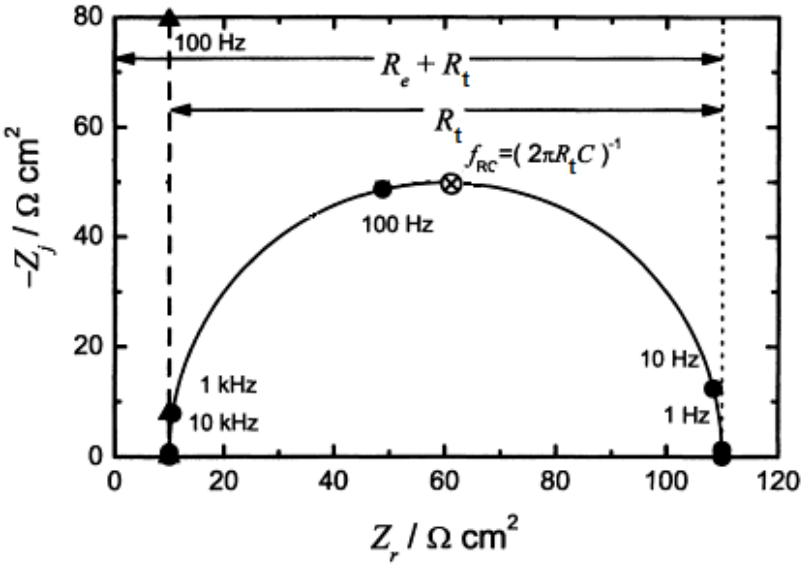

Figure 2-3. Impedance representation for the system in Figure 2-1 where $R_e = 10\ \Omega\ cm^2$, $R_t = 100\ \Omega\ cm^2$, and $C = 10\ \mu F/cm^2$. Here f_{RC} is representing the characteristic frequency

Impedance data, which are obtained from various oscillating frequencies, are represented on a complex plane, which is known as the Nyquist plot. Figure 2-3 shows a typical impedance response plot corresponding to the circuit in Figure 2-1.[6]

CHAPTER 3
EXPERIMENTAL METHOD

Electrochemical experiments were performed on commercial $LiCoO_2$ coin cells. Impedance spectroscopy was used to monitor changes associated with different states-of-charge, imposition of overcharge, and imposition of overdischarge.

3.1 Coin Cells

Commercial secondary 2032 button (or coin) cells were purchased from AA Portable Power Corp. (Richmond, CA, http://www.batteryspace.com). The 2032 specification means that the batteries were 20 mm in diameter and 3.2 mm in height. The cathode was LiCoO2, the separator was Celgard 8 μm and the anode was carbon. The normal potential range of the cells is between 3.00 and 4.20 volts.

3.2 Instrumentation

Electrochemical and impedance experiments were performed using a Gamry PCI4/750 Potentiostat connected to a desktop computer. Gamrys Virtual Front Panel (VFP600) and Electrochemical Impedance Spectroscopy (EIS300) software packages were employed. The primary purpose of the potentiostat in these experiments was to maintain a constant cell potential while measuring the impedance.

3.3 Protocol

The impedance response was analyzed overcharge and overdischarge profiles. The $LiCoO_2$ cells were initially charged under galvanostatic control to 3.80 V. Each cell was potentiostatically held at constant cell potential. After the constant-potential rest period, the impedance was measured using a 10 mV perturbation and 100 kHz - 0.02 Hz frequency range. Lissajous plots were used to ensure linearity during the impedance measurement.[8] Following each impedance measurement, the cell potential was

potentiostatically modified for the charge and discharge pro files in 0.20 V steps. In the same manner, the discharge profile analysis was executed immediately following the charge schedule. The software incorporated in the Gamry system enabled consistent and precise procedures to be performed which served to reduce errors among the repetitive experiments. In addition, the effect of overcharging a $LiCoO_2$ cell was analyzed. The cell was initially charged under constant current to 4.20 V. As before, a 10 mV ac perturbation and 100 kHz - 0.02 Hz frequency range were implemented. Impedance measurements were performed at each 80 mV step up to and including 5.00 V. A similar protocol was followed for the overdischarge. Impedance measurements were performed at each 80 mV step down to and including 2.20 V.

All experiments were performed at room temperature (around 20 ^{o}C), and they were repeated a few times with same type of battery cells to ensure that the results were both consistent and reproducible.

CHAPTER 4
RESULTS AND DISCUSSIONS OF EXPERIMENTS

The impedance responses of the $LiCoO_2$ coin cells are presented for normal operation, overcharge, and overdischarge conditions. To elucidate the sources of changes seen in impedance results, impedance measurements were also made as a function of elapsed time.

4.1 Normal Operation

The impedance response for two commercial $LiCoO_2$ coin cells is presented in Figure 4-1 with cell potential from 3.0 to 4.2 V as a parameter. These results represent the impedance response under normal operating conditions.

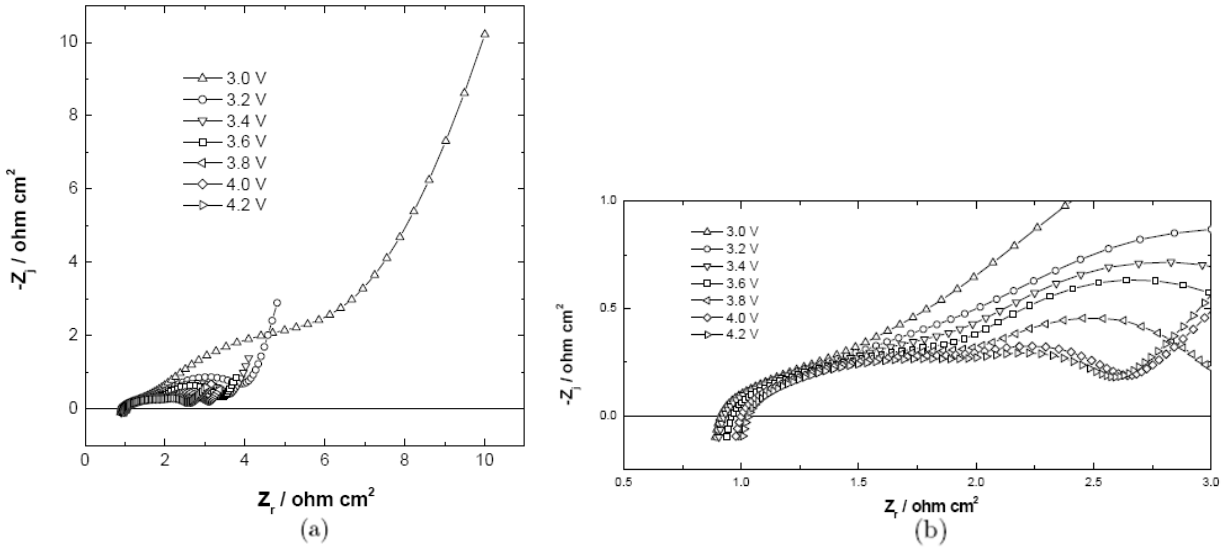

Figure 4-1. Impedance response in Nyquist format for two $LiCoO_2$ coin cells under normal operating conditions with cell potential as a parameter: a) included whole frequency and b) with zooming into high frequencies

4.2 Overcharge

To explore the sensitivity of impedance spectroscopy to overcharging the battery, the coin cell potential was increased in 80 mV increments and the impedance was measured after the cell current approached zero. The impedance is a strong function of

cell potential. To make the features visible, the impedance response is presented in a sequence of plots. The impedance response is presented in Figure 4-2 for cell potential ranging from 4.20 to 4.44 V (Figure 4-2(a)) and potential ranging from 4.44 to 4.60 V (Figure 4-2(b)).

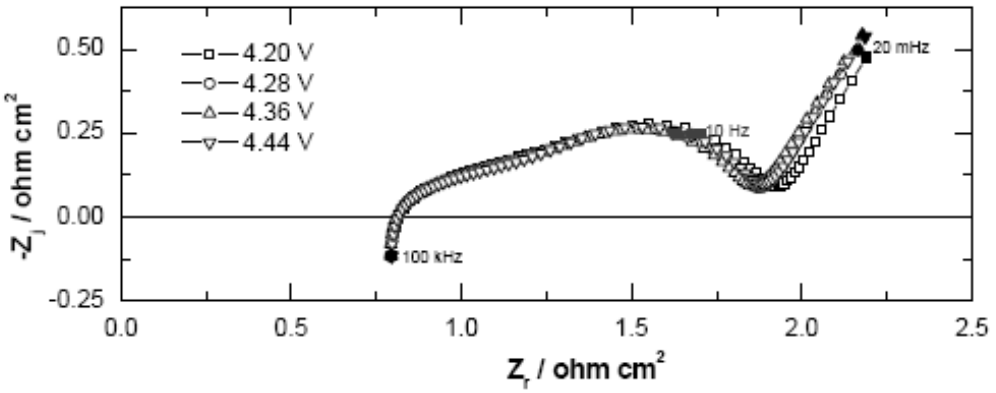

(a)

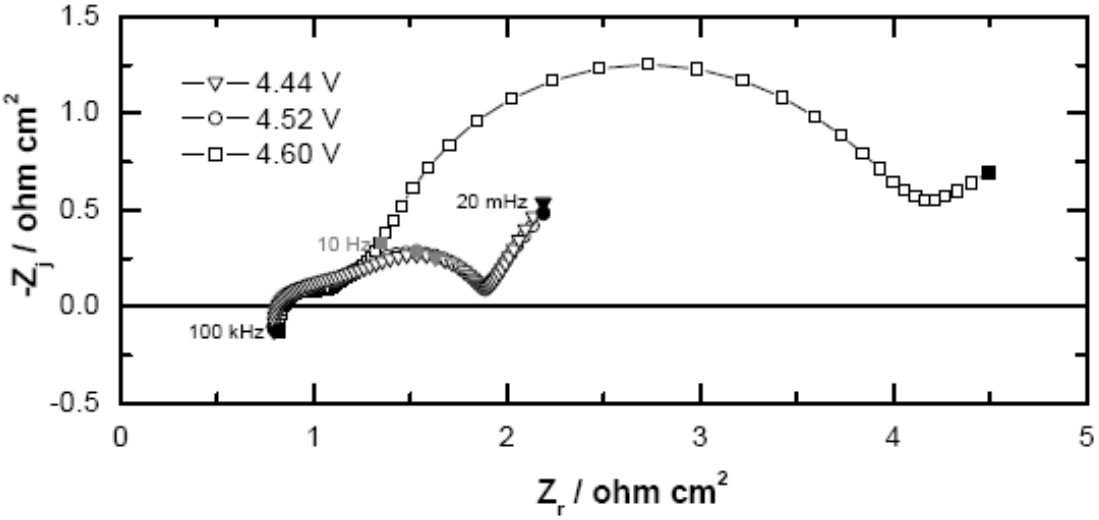

(b)

Figure 4-2. Impedance response in Nyquist format for a $LiCoO_2$ coin cell under overcharge conditions with cell potential as a parameter: a) potential ranging from 4.20 to 4.44 V; and b) potential ranging from 4.44 to 4.60 V

The impedance response is presented in Figure 4-3 for cell potential ranging from 4.60 to 4.76 V (for whole frequency range Figure 4-3(a) and for zooming into high frequencies Figure 4-3(b)).

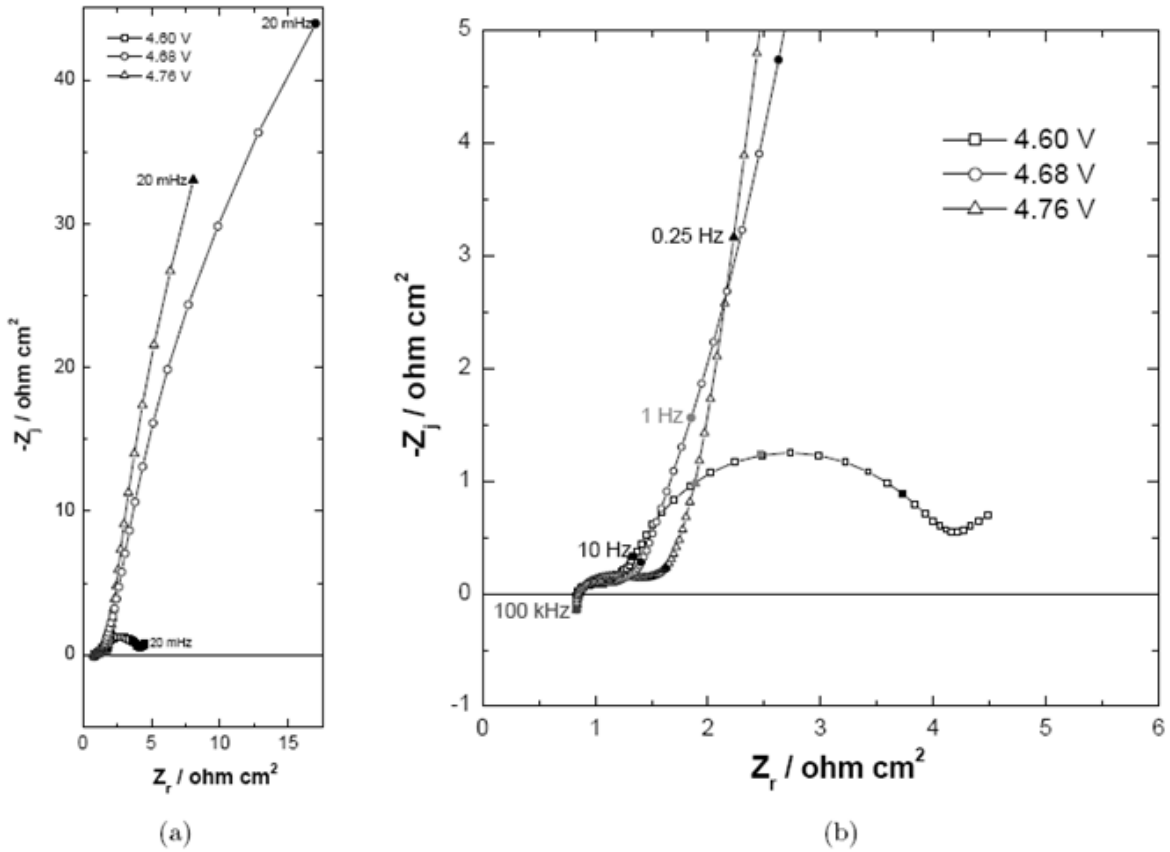

Figure 4-3. Impedance response in Nyquist format for a $LiCoO_2$ coin cell under overcharge conditions with cell potential as a parameter: a) potential ranging from 4.60 to 4.76 V; and b) with zooming into high frequencies

The impedance response is presented in Figure 4-4 potential ranging from 4.76 to 5.00 V (for whole frequency range Figure 4-4(a) and for zooming into high frequencies Figure 4-4(b)).

The results indicate that, for potentials above 4.6 V, the low-frequency impedance increases very sharply.

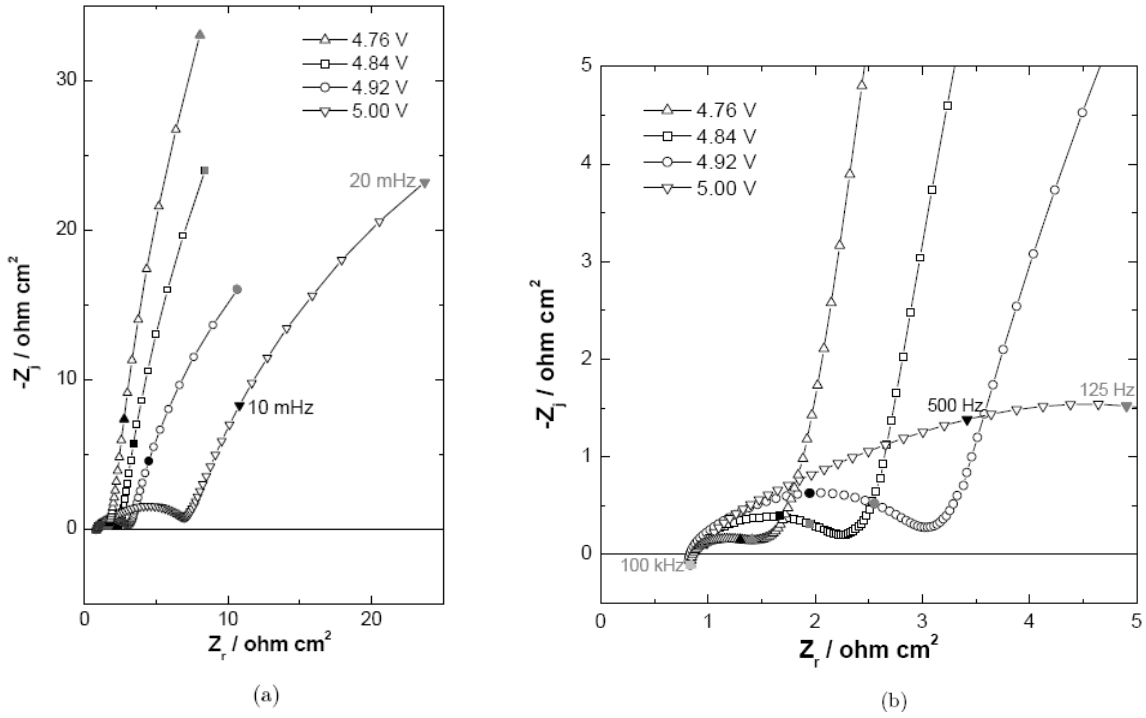

Figure 4-4. Impedance response in Nyquist format for a $LiCoO_2$ coin cell under overcharge conditions with cell potential as a parameter: a) potential ranging from 4.76 to 5.00 V; and b) with zooming into high frequencies

After overcharging to a potential of 5 V, the battery was allowed to relax for two days at the open-circuit condition. When held at open-circuit, the overcharged battery rapidly reached a cell potential within the nominal operating range, as shown in Figure 4-5.

During self-discharge, randomly taken impedance measurements were shown in Figure 4-6 whose response remains extensive and has very small differences with time (for whole frequency range Figure 4-6(a) and for zooming into high frequencies Figure 4-6(b)).

While the resulting potential was well within the nominal operating range, the impedance response measured before and after the cell was overcharged, presented in Figure 4-7, shows dramatic differences.

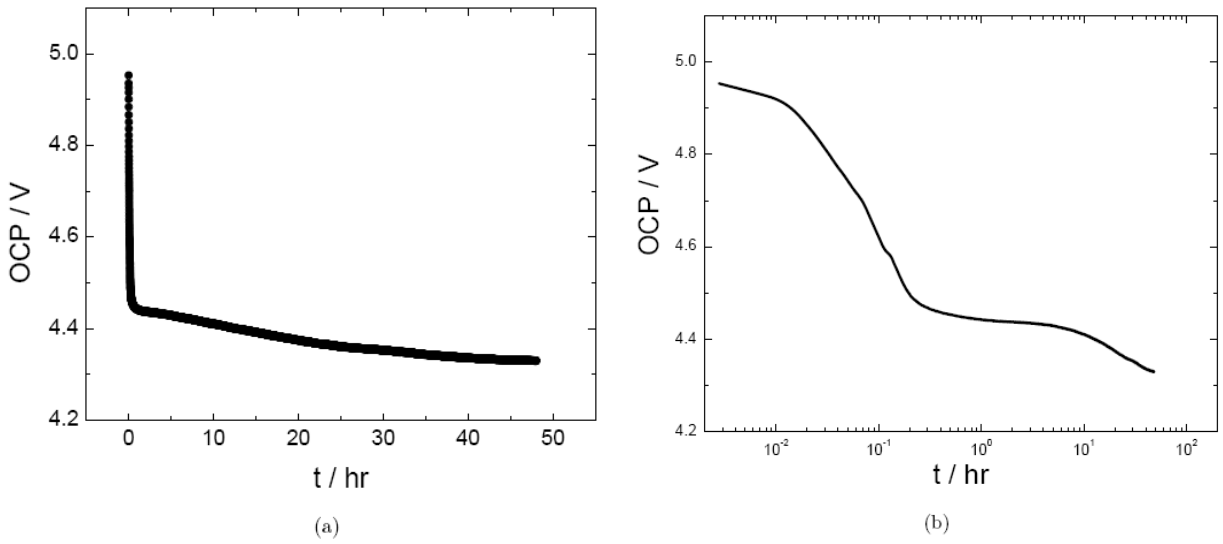

Figure 4-5. Open-circuit potential as a function of time for an overcharged cell: a) in normal scale and b) in semi-logarithmic scale

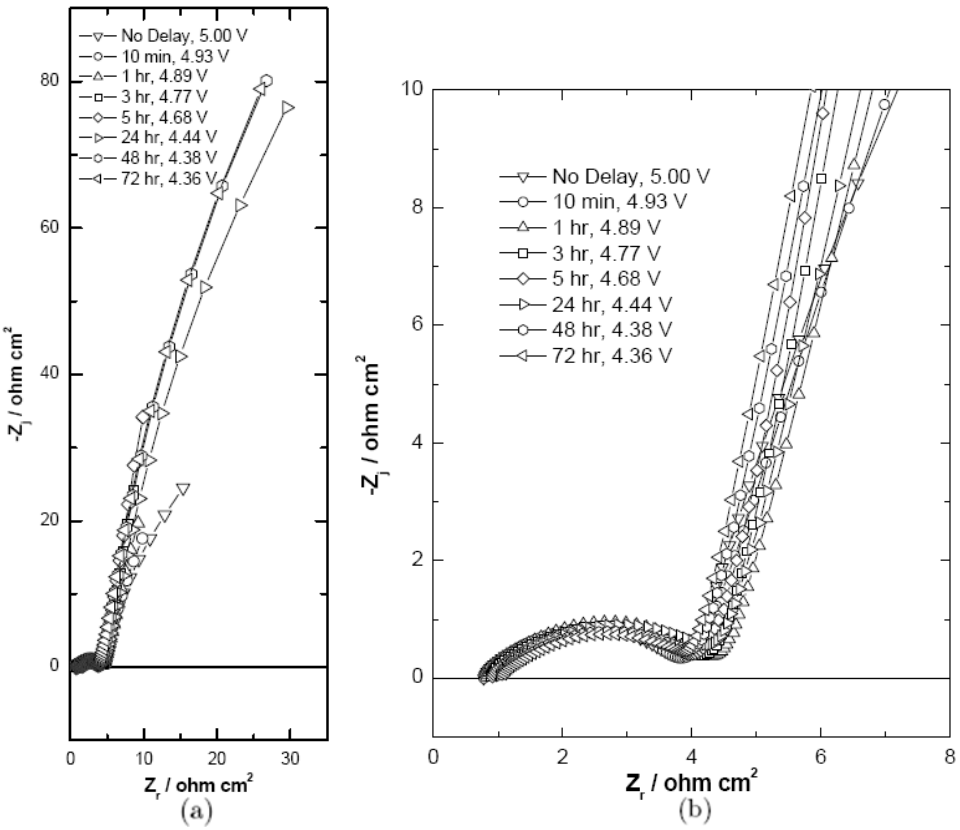

Figure 4-6. Impedance response in Nyquist format for a $LiCoO_2$ coin cell during self-discharge under overcharge conditions with elapsed time as a parameter: a) included whole frequencies and b) with zooming into high frequencies

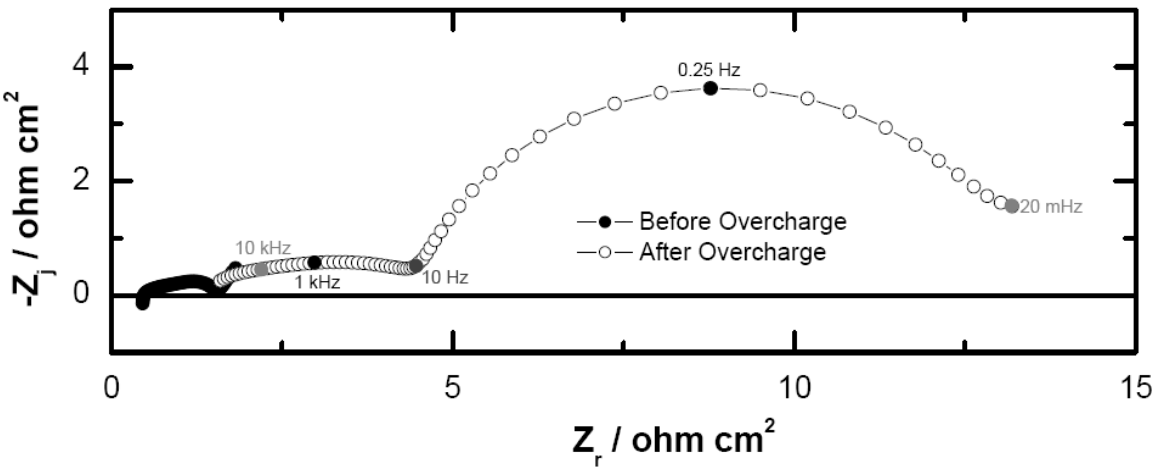

Figure 4-7. Impedance response of a button cell at a potential of 4 V before and after the cell was overcharged

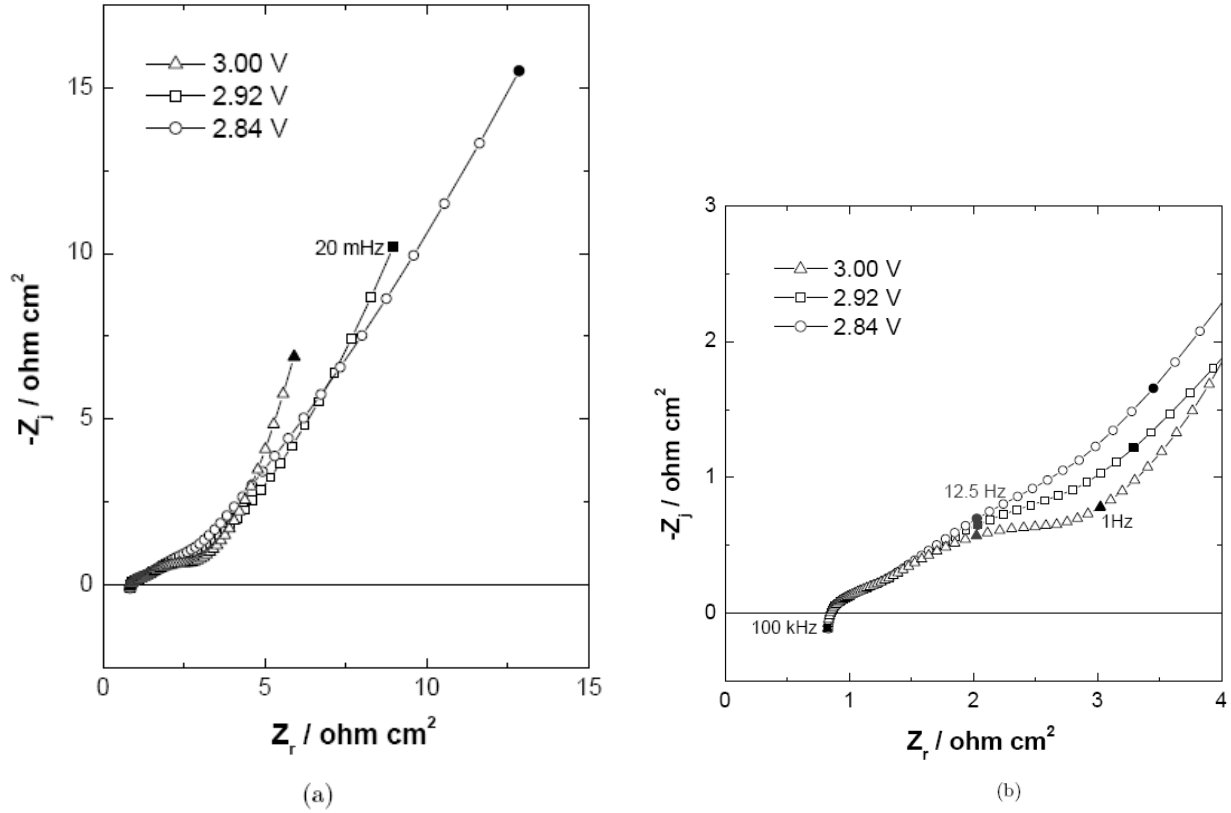

Figure 4-8. Impedance response in Nyquist format for a $LiCoO_2$ coin cell under overdischarge conditions with cell potential as a parameter: a) potential ranging from 3.00 to 2.84 V; and b) with zooming into high frequencies

4.3 Overdischarge

To explore the sensitivity of impedance spectroscopy to over discharging the battery, the coin cell potential was decreased in 80 mV increments and the impedance was measured after the cell current approached zero. The impedance is again a strong function of cell potential. To make the features visible, the impedance response is presented in a sequence of plots. The impedance response is presented in Figure 4-8 for cell potential ranging from 3.00 to 2.84 V (for whole frequency range Figure 4-8(a) and for zooming into high frequencies Figure 4-8(b)).

The impedance response is presented in Figure 4-9 for cell potential ranging from 2.84 to 2.60 V (Figure 4-9(a)) and potential ranging from 2.60 to 2.36 V (Figure 4-9(b)).

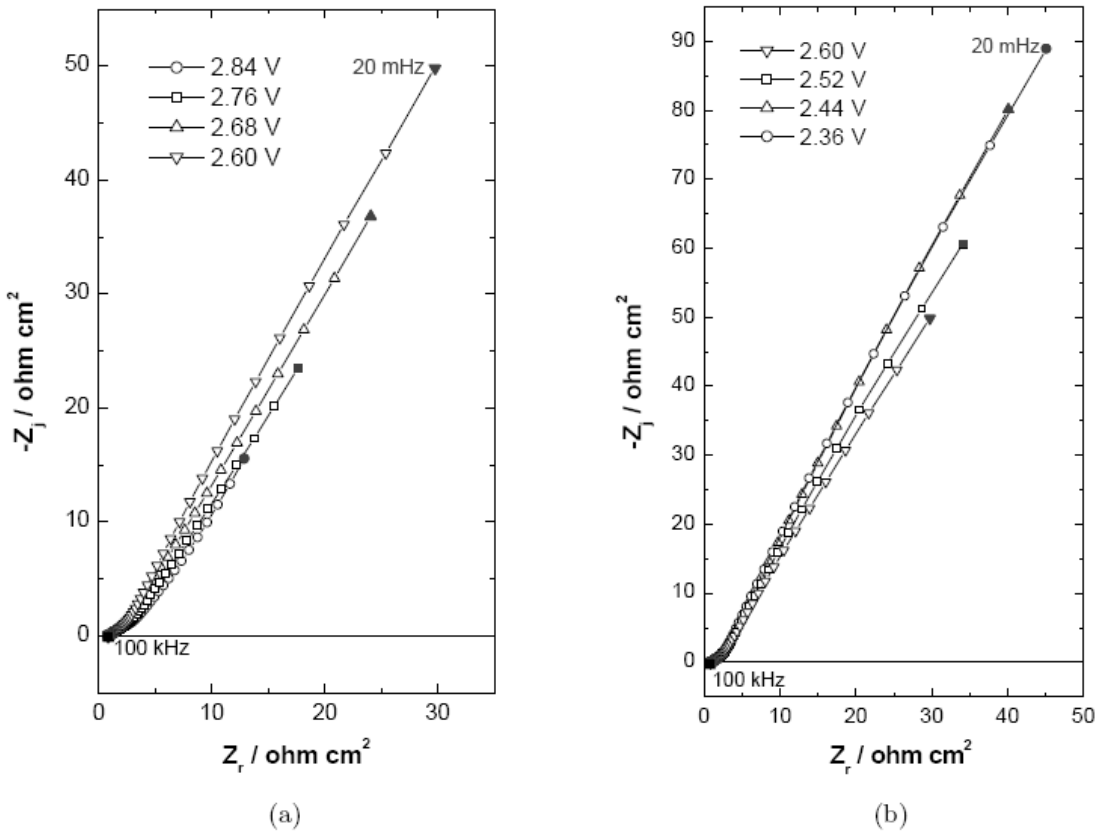

Figure 4-9. Impedance response in Nyquist format for a $LiCoO_2$ coin cell under overdischarge conditions with cell potential as a parameter: a) potential ranging from 2.84 to 2.60 V; and b) potential ranging from 2.60 to 2.36 V

Finally, the impedance response is presented in Figure 4-10 for cell potential ranging from 2.36 to 2.20 V.

After overdischarging to a potential of 2.20 V, the battery was allowed to relax for two days at the open-circuit condition. When held at open-circuit, the overdischarged battery slowly reached a cell potential within the nominal operating range, as shown in Figure 4-11.

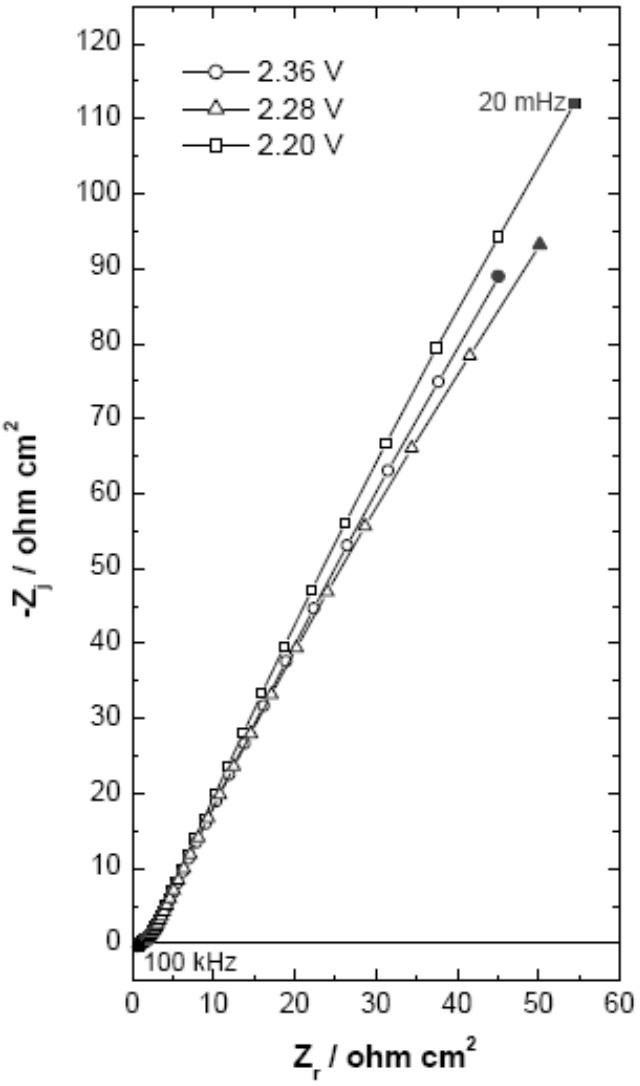

Figure 4-10. Impedance response in Nyquist format for a $LiCoO_2$ coin cell under overdischarge conditions with potential ranging from 2.36 to 2.20 V

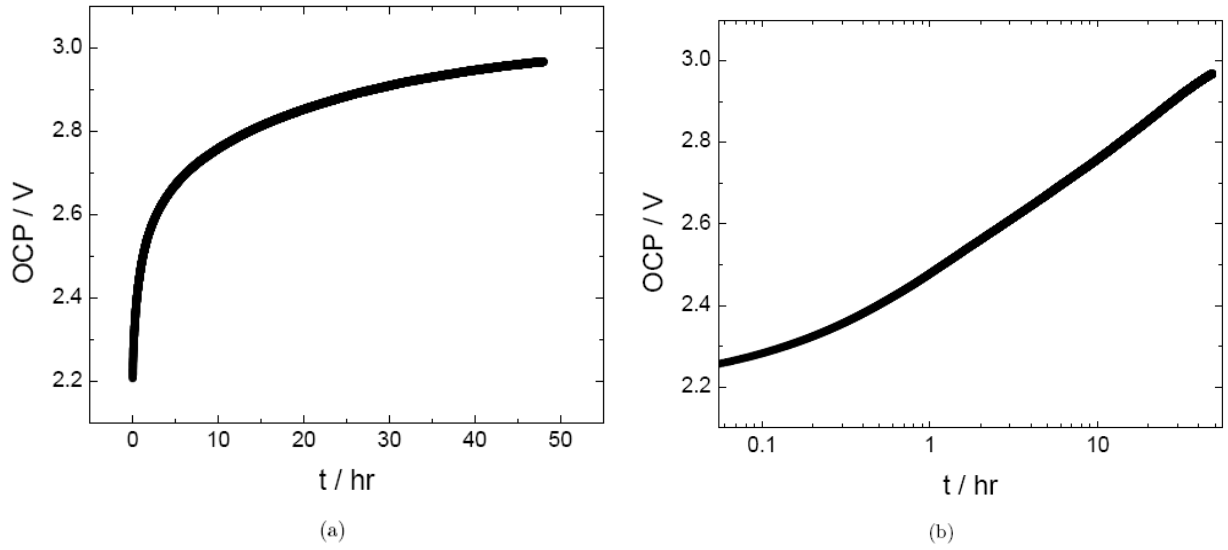

Figure 4-11. Open-circuit potential as a function of time for an overdischarged cell: a) in normal scale and b) in semi-logarithmic scale

During self-charge, randomly taken impedance measurements were shown in Figure 4-12. The response remains extensive until a certain time, and then it recovers itself by getting the smaller impedance values with reaching the nominal range (for whole frequency range Figure 4-12(a) and for zooming into high frequencies Figure 4-12(b)).

In contrast to the results seen for the overcharged battery (Figure 4-7), the impedance response measured before and after the cell was overdischarged, presented in Figure 4-13, showed only minor differences in the Ohmic resistance.

4.4 Influence of Elapsed Time

To explore whether the differences in the impedance response shown in Figure 4-13 for the cell before and after over-discharge could be attributed to elapsed time, a sequence of impedance measurements were made at a potential of 4 V. The resulting impedance spectra are shown in Figure 4-14 with elapsed time as a parameter.

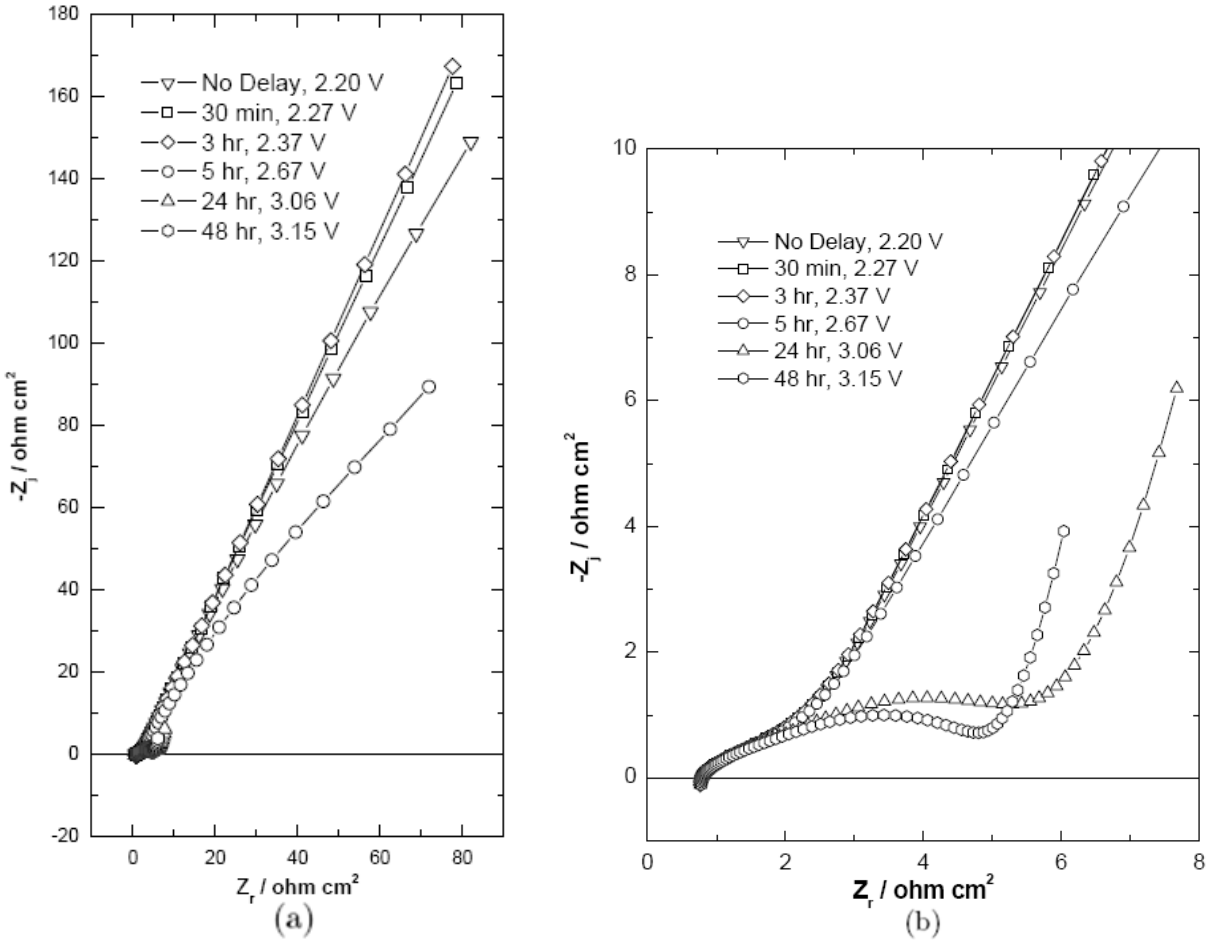

Figure 4-12. Impedance response in Nyquist format for a $LiCoO_2$ coin cell during self-charge under overdischarge conditions with elapsed time as a parameter: a) included whole frequencies and b) with zooming in greater frequencies

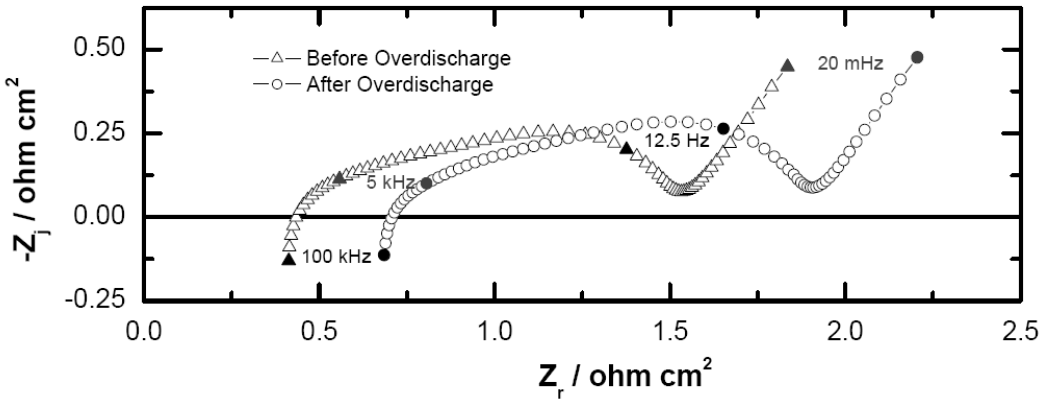

Figure 4-13. Impedance response of a button cell at a potential of 4 V before and after the cell was overdischarged

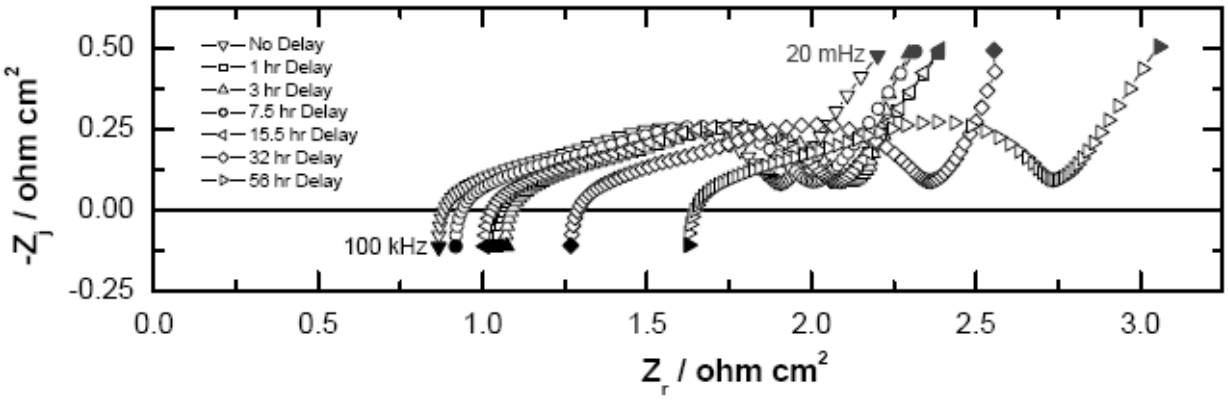

Figure 4-14. Impedance response of a button cell at a potential of 4 V with elapsed time as a parameter

CHAPTER 5
MEASUREMENT MODEL ANALYSIS

A measurement model analysis was employed to extract physically meaningful parameters. A graphical analysis was used to show that the change in the impedance response with elapsed time was due to a change in the Ohmic resistance.

5.1 Measurement Model

As described by Orazem,[9] the measurement model was introduced as a means to resolve recurring issues in regression of impedance data, e.g.,[10,11,12]

1. identification of the most appropriate weighting strategy for regression,
2. assessment of the noise level in the measurement, and
3. identification of the frequency range unaffected by instrumental artifacts or non-stationary behavior.

A distinction is drawn, following Agarwal et al.,[10,11,12] between stochastic errors that are randomly distributed about a mean value of zero, errors caused by the lack of fit of a model, and experimental bias errors that are propagated through the model. The experimental bias errors, assumed to be those that cause lack of consistency with the Kramers-Kronig relations,[13,14,15] may be caused by non-stationarity or by instrumental artifacts. The problem of interpretation of impedance data is therefore defined to consist of two parts: one of identification of experimental errors, which includes assessment of consistency with the Kramers-Kronig relations, and one of fitting, which entails model identification, selection of weighting strategies, and examination of residual errors. The error analysis provides information that can be incorporated into regression of process models.

The measurement model method for distinguishing between bias and stochastic errors is based on using a generalized model as a filter for non-replicacy of impedance

data. The measurement model is composed of a superposition of line-shapes which can be arbitrarily chosen subject to the constraint that the model satisfies the Kramers-Kronig relations. The model composed of Voigt elements in series with a solution resistance has been shown to be a useful measurement model. With a sufficient number of parameters, the Voigt model was able to provide a statistically significant fit to a broad variety of impedance spectra.[10]

The measurement model is used first to filter lack of replication of repeated impedance scans. The statistics of the residual errors yields an estimate for the variance (or standard deviation) of stochastic measurement errors. This experimentally-determined variance is then used to weight subsequent regression of the measurement model to determine consistency with the Kramers-Kronig relations. If the data can be represented by a model that is itself consistent with the Kramers-Kronig relations, the data can be considered to be consistent. The concept of using a generalized measurement model to assess consistency with the Kramers-Kronig relations, first introduced by Agarwal et al.,[10, 12,16] was also employed by Boukamp and Macdonald[17] and by Boukamp[18] using weighting strategies based on an assumed error structure. The experimental determination of the stochastic error structure as used here, however, allows formal quantification of the extent of agreement with the Kramers-Kronig relations. Other transfer-function models can be used as a measurement model so long as they are consistent with the Kramers-Kronig relations. Shukla and Orazem have demonstrated that the stochastic error structure determined from replicated impedance measurements is independent of the type of measurement model used.[19] While the regressed parameters may not be associated unequivocally with a set of deterministic

or theoretical parameters for a given system, the measurement model approach has been shown to represent adequately the impedance spectra obtained for a large variety of electrochemical systems.[10] Regardless of their interpretation, the measurement model representation can be used to filter and thus identify the non-stationary (drift) and high-frequency (noise) components contained in an impedance spectrum.

The measurement model has been applied in previous works to assess the error structure of a variety of systems including electrohydrodynamic impedance,[20] electrochemical impedance data for reduction of ferricyanide on a Pt rotating disk,[21] for corrosion of cast iron in Evian water,[22] for corrosion of aluminum in orange juice,[9] for charging of electroactive polymers,[23] and for analysis of PEM fuel cells.[24, 25] Here the error analysis approach is applied to electrochemical impedance data collected for lithium-ion batteries.

5.2 Measurement Model Results

The measurement model was used to assess the high-frequency asymptote for the real part of the impedance. This term is the Ohmic resistance for the cell. A truncated data set was used to estimate the charge-transfer resistance for the high-frequency capacitive loop. A sample of the fitting results is shown in Figure 5-1.

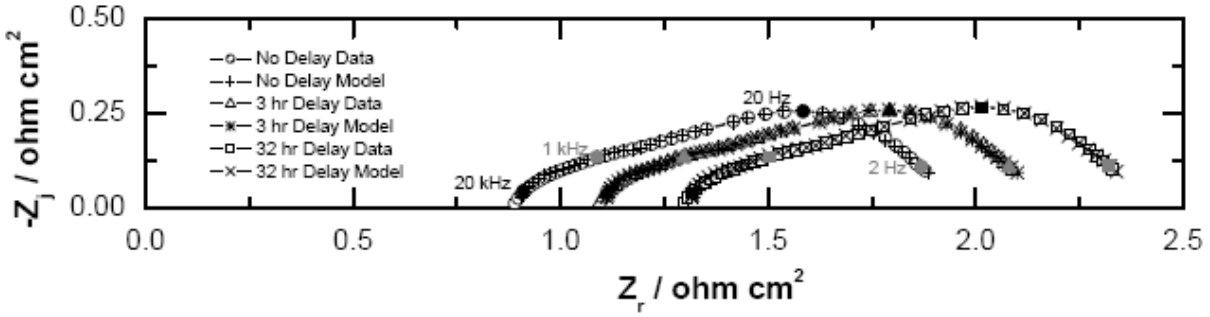

Figure 5-1. Measurement model analysis for the impedance response of a button cell at a potential of 4 V with elapsed time as a parameter

The resulting values for Ohmic and charge-transfer resistance are shown in Figure 5-2 as a function of elapsed time. The charge-transfer resistance is independent of time, but the Ohmic resistance increases with time.

The effect can be demonstrated by plotting a scaled impedance in which $-Z_j/R_t$ is plotted as a function of $(Z_r-R_e)/R_t$. The results, presented in Figure 5-3, show that the shape of the capacitive loop is unaffected by the passage of time. The superposition of impedance curves shows that there were no mechanistic changes in the electrochemical reactions, and that the change in the impedance response with elapsed time can be attributed solely to a change in the Ohmic resistance.

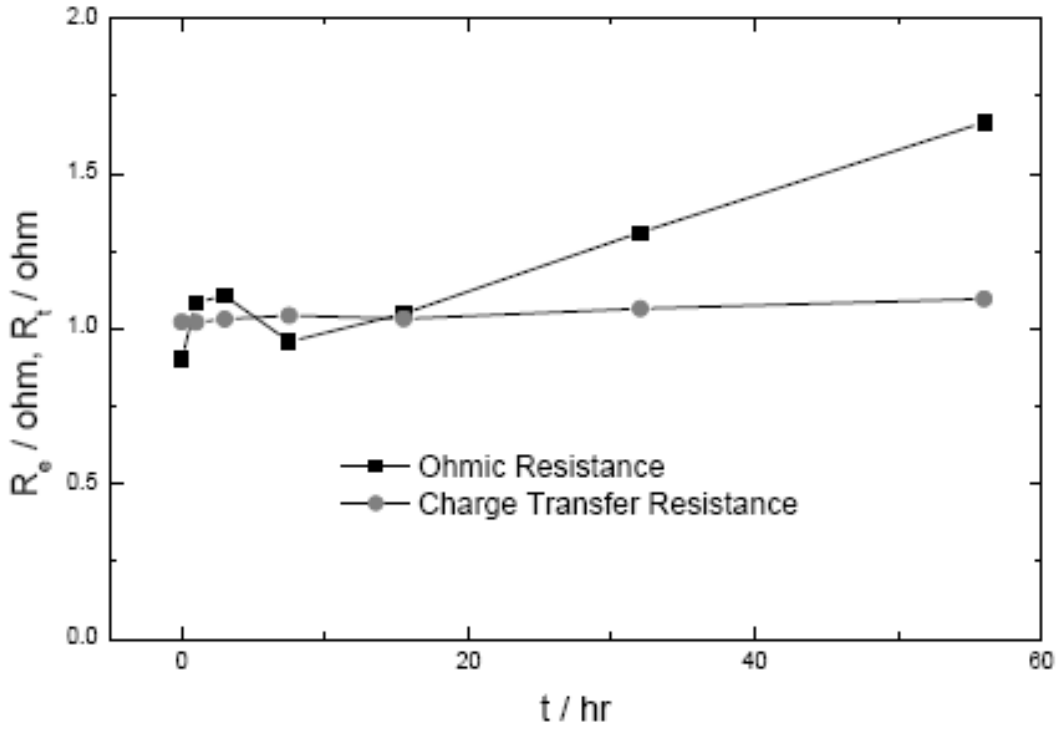

Figure 5-2. Ohmic and charge transfer resistance obtained from the measurement model analysis of the data presented in Figure 4-14 as a function of elapsed time

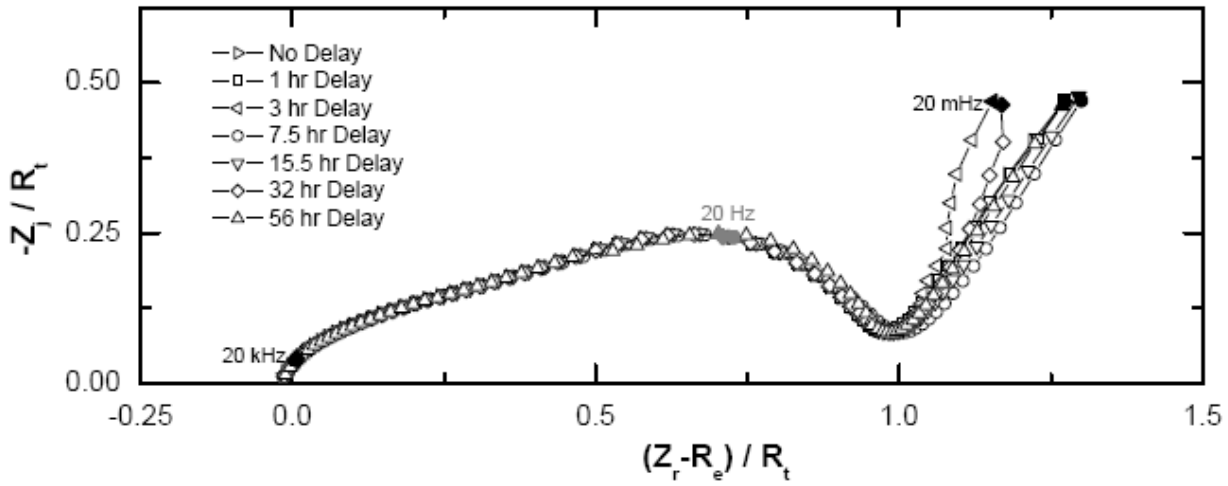

Figure 5-3. Scaled impedance response of a button cell at a potential of 4 V with elapsed time as a parameter

CHAPTER 6
CONCLUSIONS

The impedance response was demonstrated to be very sensitive to the history of a lithium-ion button cell. The impedance increases dramatically when the battery is either overcharged or overdischarged. When the battery is held at open circuit, the cell returns to a potential within the nominal normal operating range. When the battery had been overcharged, the impedance remains much larger than it was originally. When the battery had been overdischarged, the impedance is essentially the same as it was originally. Any differences in impedance response were attributed to passage of time.

LIST OF REFERENCES

[1] M. Winter and R. J. Brodd, “What Are Batteries, Fuel Cells, and Supercapacitors?” Chemical Reviews, 104 (2004) 4245–4270.

[2] M. Urquidi-Macdonald and N. A. Bomberger, “Predicting Failure of Secondary Batteries,” Journal of Power Sources, 74 (1998) 87–98.

[3] S. B. Peterson, J. Apt, and J. Whitacre, “Lithium-Ion Battery Cell Degradation Resulting from, Realistic Vehicle and Vehicle-To-Grid Utilization,” Journal of Power Sources, 195 (2010) 2385–2392.

[4] H. Maleki and J. N. Howard, “Effects of Overdischarge on Performance and Thermal Stability of a Li-Ion Cell,” Journal of Power Sources, 160 (2006) 1395–1402.

[5] D. Belov and M.-H. Yang, “Failure Mechanism of Li-Ion Battery at Overcharge Conditions,” Journal of Solid State Electrochemistry, 12 (2008) 885–894.

[6] M. E. Orazem and B. Tribollet, “Electrochemical Impedance Spectroscopy,” John Wiley & Sons Inc.,(2008) 310-313.

[7] S. Wu, “Influence of Electrode Geometry on Local and Global Impedance Response,” University of Florida PhD thesis, (2010), 27-29.

[8] B. Hirschorn, B. Tribollet, and M. E. Orazem, “On Selection of the Perturbation Amplitude Required to Avoid Nonlinear Effects in Impedance Measurements,” Israel Journal of Chemistry, 48 (2008) 133–142.

[9] M. E. Orazem, “A Systematic Approach toward Error Structure Identification for Impedance Spectroscopy,” Journal of Electroanalytical Chemistry, 572 (2004) 317–327.

[10] P. Agarwal, O. D. Crisalle, M. E. Orazem, and L. H. García-Rubio, “Measurement Models for Electrochemical Impedance Spectroscopy: I. Demonstration of Applicability,” Journal of the Electrochemical Society, 139 (1992) 1917–1927.

[11] P. Agarwal, O. D. Crisalle, M. E. Orazem, and L. H. García-Rubio, “Measurement Models for Electrochemical Impedance Spectroscopy: II. Determination of the Stochastic Contribution to the Error Structure,” Journal of the Electrochemical Society, 142 (1995) 4149–4158.

[12] P. Agarwal, O. D. Crisalle, M. E. Orazem, and L. H. García-Rubio, “Measurement Models for Electrochemical Impedance Spectroscopy: III. Evaluation of Consistency with the Kramers-Kronig Relations,” Journal of the Electrochemical Society, 142 (1995) 4159–4168.

[13] R. de L. Kronig, On the Theory of Dispersion of X-Rays," Journal of the Optical Society of America and Review of Scientific Instruments, 12 (1926) 547–557.

[14] R. de L. Kronig, "Dispersionstheorie im Röntgengebeit," Phys. Zs., 30 (1929) 521–522.

[15] H. A. Kramers, "Die Dispersion und Adsorption von Röntgenstrahlen," Phys. Zs., 30 (1929) 522–523.

[16] P. Agarwal, M. E. Orazem, and L. H. García-Rubio, "Application of the Kramers-Kronig Relations to Electrochemical Impedance Spectroscopy," in Electrochemical Impedance : Analysis and Interpretation, J. Scully,D. Silverman, and M. Kendig, editors, volume ASTM STP 1188 (Philadelphia, PA: American Society for Testing and Materials, 1993) 115–139.

[17] B. A. Boukamp and J. R. Macdonald, "Alternatives to Kronig-Kramers Transformation and Testing, and Estimation of Distributions," Solid State Ionics, 74 (1994) 85–101.

[18] B. A. Boukamp, "A Linear Kronig-Kramers Transform Test for Immittance Data Validation," Journal of the Electrochemical Society, 142 (1995) 1885–1894.

[19] P. K. Shukla, M.E. Orazem, and O. D. Crisalle, "Validation of the Measurement Model Concept for Error Structure Identification," Electrchimica Acta, 49 (2004) 2881–2889.

[20] M.E. Orazem, P. Agarwal, C. Deslouis, and B. Tribollet, "Application of Measurement Models to Electrohydrodynamic Impedance Spectroscopy," Journal of the Electrochemical Society, 143 (1996) 948–960.

[21] M. E. Orazem, M. Durbha, C. Deslouis, H. Takenouti, and B. Tribollet, "Influence of Surface Phenomena on the Impedance Response of a Rotating Disk Electrode," Electrochimica Acta, 44 (1999) 4403–4412.

[22] I. Frateur, C. Deslouis, M. E. Orazem, and B. Tribollet, "Modeling of the Cast Iron/Drinking Water System by Electrochemical Impedance Spectroscopy," Electrochimica Acta, 44 (1999) 2087–2093.

[23] C. Deslouis, T. E. Moustafid, M. M. Musiani, M. E. Orazem, V. Provost, and B. Tribollet, "Effect of Cations on the Diffusivity of the Charge Carriers in Polyaniline Membranes," Electrochimica Acta, 44 (1999) 2087–2093.

[24] S. K. Roy and M. E. Orazem, "Error Analysis for the Impedance Pesponse of PEM Fuel Cells," Journal of the Electrochemical Society, 154 (2007) B883–B891.

[25] S. K. Roy and M. E. Orazem, "Analysis of Flooding as a Stochastic Process in Polymer Electrolyte Membrane (PEM) Fuel Cells by Impedance Techniques," Journal of Power Sources, 184 (2008) 212–219.

BIOLOGICAL SKETCH

Salim Erol received his Bachelor of Science degree in chemical engineering from Eskisehir Osmangazi University in June of 2006. Then he began a master's program at Marmara University in Turkey. While he was preparing his master's thesis, he applied for a government scholarship, and he was chosen as a scholar for his master's and his Ph.D. Consequently, he had to leave his program in Turkey, in order to make a new start toward a master's degree and Ph.D. from an American university. To reach a sufficient level in English, he studied at an English-language school, the English Programs for Internationals at the University of South Carolina, and finished the school in April of2009. After, he entered the University of Florida as a master's student in the chemical engineering department in August of 2009. He has been in the electrochemical impedance research group, under the direction of Professor Mark Orazem, since January of 2010.